



Sex-dependent Effects of Developmental Hypoxia on Cardiac Mitochondria from Adult Murine Offspring

DOI:

[10.1016/j.freeradbiomed.2020.11.004](https://doi.org/10.1016/j.freeradbiomed.2020.11.004)

Document Version

Accepted author manuscript

[Link to publication record in Manchester Research Explorer](#)

Citation for published version (APA):

Hellgren, K., Premanandhan, H., Quinn, C., Trafford, A., & Galli, G. (2020). Sex-dependent Effects of Developmental Hypoxia on Cardiac Mitochondria from Adult Murine Offspring. *Free Radical Biology and Medicine*. <https://doi.org/10.1016/j.freeradbiomed.2020.11.004>

Published in:

Free Radical Biology and Medicine

Citing this paper

Please note that where the full-text provided on Manchester Research Explorer is the Author Accepted Manuscript or Proof version this may differ from the final Published version. If citing, it is advised that you check and use the publisher's definitive version.

General rights

Copyright and moral rights for the publications made accessible in the Research Explorer are retained by the authors and/or other copyright owners and it is a condition of accessing publications that users recognise and abide by the legal requirements associated with these rights.

Takedown policy

If you believe that this document breaches copyright please refer to the University of Manchester's Takedown Procedures [<http://man.ac.uk/04Y6Bo>] or contact uml.scholarlycommunications@manchester.ac.uk providing relevant details, so we can investigate your claim.



1 **Sex-dependent Effects of Developmental Hypoxia on Cardiac Mitochondria**
2 **from Adult Murine Offspring**

3

4 Kim T. Hellgren¹, Hajani Premanandhan¹, Callum J. Quinn¹, Andrew W Trafford¹
5 and Gina L. J. Galli*¹

6

7 ¹Division of Cardiovascular Sciences, School of Medical Sciences, University of
8 Manchester, Manchester M13 9NT, UK

9

10 *Corresponding Author

11 **Dr Gina Galli**

12 Division of Cardiovascular Sciences,

13 School of Medical Sciences,

14 University of Manchester,

15 3.09 Core Technology Facility,

16 46 Grafton St,

17 Manchester M13 9NT, UK

18 gina.galli@manchester.ac.uk

19 **Abstract**

20 Insufficient oxygen supply (hypoxia) during fetal and embryonic development can lead to
21 latent phenotypical changes in the adult cardiovascular system, including altered cardiac
22 function and increased susceptibility to ischemia reperfusion injury. While the cellular
23 mechanisms underlying this phenomenon are largely unknown, several studies have
24 pointed towards metabolic disturbances in the heart of offspring from hypoxic
25 pregnancies. To this end, we investigated mitochondrial function in the offspring of a
26 mouse model of prenatal hypoxia. Pregnant C57 mice were subjected to either normoxia
27 (21%) or hypoxia (14%) during gestational days 6-18. Offspring were reared in normoxia
28 for up to 8 months and mitochondrial biology was assessed with electron microscopy
29 (ultrastructure), spectrophotometry (enzymatic activity of electron transport chain
30 complexes), microrespirometry (oxidative phosphorylation and H₂O₂ production) and
31 Western Blot (protein expression). Our data showed that male adult offspring from
32 hypoxic pregnancies possessed mitochondria with increased H₂O₂ production and lower
33 respiratory capacity that was associated with reduced protein expression of complex I, II
34 and IV. In contrast, females from hypoxic pregnancies had a higher respiratory capacity
35 and lower H₂O₂ production that was associated with increased enzymatic activity of
36 complex IV. From these results, we speculate that early exposure to hypoxia has long
37 term, sex-dependent effects on cardiac metabolic function, which may have implications
38 for cardiovascular health and disease in adulthood.

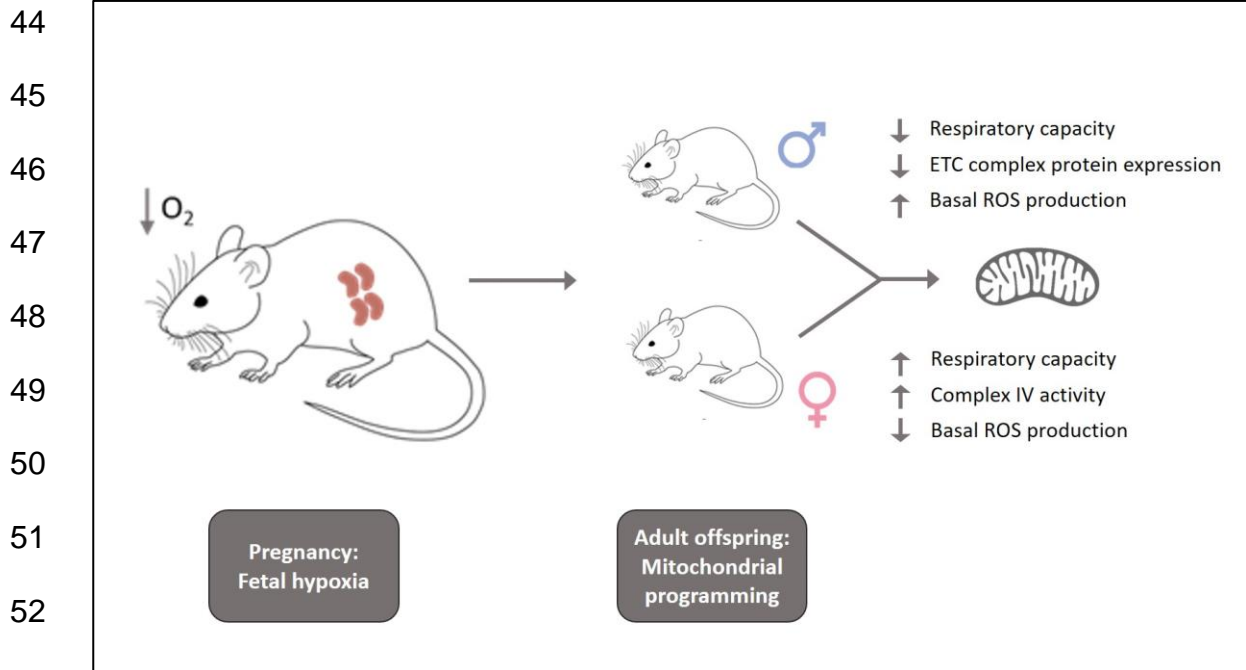
39

40

41

42

43 **Graphical Abstract**



53

54

55

56 **Keywords**

57 Heart

58 Mitochondria

59 Developmental programming

60 Fetal hypoxia

61 Reactive oxygen species

62

63

64

65

66

67 **Abbreviations**

68 ADP - adenosine diphosphate

69 CS - citrate synthase

70 ETC – electron transport chain

71 ET_{CI+CII} - electron transfer capacity with complex I and II substrates

72 ET_{CII} - electron transfer capacity with complex II substrates

73 FCCP - carbonyl cyanide-4-(trifluoromethoxy)phenylhydrazone

74 GD – gestational day

75 H_2O_2 – hydrogen peroxide

76 HRP - horseradish peroxidase

77 I/R – ischemia reperfusion

78 $LEAK_{CI}$ - Leak respiratory state with complex I substrates

79 MPG - malate pyruvate and glutamate

80 O_2^- - superoxide

81 OXPHOS – oxidative phosphorylation

82 $OXPHOS_{CI}$ - oxidative phosphorylation with complex I substrates

83 $OXPHOS_{CI+CII}$ - oxidative phosphorylation with complex I and II substrates

84 $PKC\epsilon$ - protein kinase C epsilon

85 RCR - respiratory control ratio

86 ROS – reactive oxygen species

87 ROX - residual non-mitochondrial oxygen consumption

88 SOD - superoxide dismutase

89 TMPD - TM/AS, N,N,N,N-tetramethyl-p-phenylenediamin

90

91 **1.0. Introduction**

92 Heart disease remains the leading cause of death worldwide ¹. Despite significant
93 advances in treatment options, prevention strategies are the most cost-effective way to
94 reduce the socioeconomic burden of these diseases. Such strategies have traditionally
95 targeted behavioral and lifestyle risk factors, such as smoking and obesity. However,
96 the seminal work of Barker ² demonstrated that adverse events during pregnancy can
97 predispose offspring to heart disease in adulthood. This phenomenon, termed
98 developmental programming, provides a window of opportunity to prevent the
99 development of heart disease in early life. Nevertheless, before effective treatments can
100 be designed, it is crucial to understand the mechanisms leading to cardiac dysfunction in
101 offspring from high-risk pregnancies.

102

103 Insufficient oxygen supply to an embryo or foetus, termed developmental hypoxia,
104 occurs in a wide range of high-risk pregnancies, including preeclampsia, placental
105 insufficiency, placental infection, maternal anaemia, gestational diabetes and high
106 altitude pregnancy ^{3,4}. Animal models have shown the foetus initially responds to
107 hypoxia by preferentially distributing blood flow to vital organs, such as the heart and
108 brain ⁴⁻⁶. While this strategy is protective in the short term, a sustained redistribution of
109 blood flow is associated with asymmetric fetal growth restriction, increased peripheral
110 resistance and cardiac abnormalities, including hypertrophy ⁴. In adulthood, the hearts
111 of offspring from hypoxic pregnancies continue to express abnormal phenotypes,
112 including diastolic dysfunction, sustained increases in myocardial contractility and
113 enhanced responsiveness to β -adrenoreceptor stimulation ⁷⁻⁹. Additionally, prenatal
114 hypoxia appears to sensitise the adult heart to ischaemia and reperfusion (I/R) injury ¹⁰⁻
115 ¹². Interestingly, females from hypoxic pregnancies appear to be partially protected

116 from cardiac dysfunction, suggesting that the effects of developmental hypoxia are
117 gender-specific ^{11,13,14}. In aggregate, these studies suggest developmental hypoxia
118 programmes a dysfunctional cardiac phenotype in offspring that cannot be reversed by
119 normalising oxygen availability after birth.

120

121 Given that most of these experiments have been conducted in isolated hearts, the
122 cardiac dysfunction in offspring from hypoxic pregnancies cannot be explained by
123 autonomic influences, altered peripheral resistance (cardiac afterload) or circulating
124 catecholamines. Therefore, the intrinsic properties of the myocardial cells have been
125 altered. While multiple cellular mechanisms may account for cardiac dysfunction, recent
126 evidence suggests intrauterine stress can alter offspring cardiac metabolism, particularly
127 at the level of the mitochondria. For example, nutritional stress during development
128 leads to a range of cardiac mitochondrial abnormalities in fetal and adult offspring,
129 including structural disorganization, impaired mitophagy, reduced oxygen consumption,
130 decreased proton leak and altered fission/fusion dynamics ¹⁵⁻¹⁷. Similarly, exposure to
131 excess glucocorticoids during development can programme cardiac mitochondrial
132 dysfunction in adult offspring, leading to increased sensitivity to ischemia/reperfusion
133 injury, higher levels of H₂O₂ production and a reduced capacity to produce ATP ¹⁸.
134 Collectively, these studies suggest mitochondrial remodeling represents a major
135 mechanism underlying the developmental programming of heart disease.

136

137 To our knowledge, only one group has investigated the long-term effects of
138 developmental hypoxia on offspring mitochondrial function. Thompson and colleagues
139 has shown pregnant guinea pigs exposed to 10.5% atmospheric oxygen between
140 gestational days (GD) 28-65 (term 65-72 days) led to sex-specific alterations in

141 mitochondrial enzymatic complex activities, mitochondrial DNA content, protein
142 expression and respiration ¹⁹⁻²². However, the moderate level of hypoxia used in these
143 studies (10.5%) caused a significant reduction in maternal weight, which is indicative of
144 nutritional stress. It is therefore difficult to conclude whether mitochondrial function is
145 being altered by developmental hypoxia or nutritional stress, or a combination of the two.
146 To this end, we have undertaken a comprehensive investigation into the effects of
147 developmental hypoxia on adult offspring mitochondrial morphology, respiratory
148 capacity, reactive oxygen species production, enzymatic activity and protein expression.
149 Our results suggest developmental hypoxia has long-term, sex-dependent effects on
150 cardiac mitochondrial function; in particular, males from hypoxic pregnancies have a
151 lower mitochondrial respiratory capacity and generate more H₂O₂ under basal conditions,
152 and females from hypoxic pregnancies have greater respiratory scope and produce less
153 H₂O₂ under basal conditions, compared to their normoxic counterparts. We speculate
154 that these phenotypes have long-term implications for metabolic health and the
155 susceptibility to heart disease.

156

157 **2.0. Methods**

158 *2.1. Animal model*

159 There are several strategies to model chronic fetal hypoxia, but most (e.g. placental
160 embolisation, reduced uterine blood flow) cause impaired placental perfusion, thereby
161 decreasing the delivery of nutrients as well as oxygen to the foetus ^{23,24}. In these
162 instances, it is difficult to separate the effects of fetal nutrient restriction versus fetal
163 hypoxia in programming cardiovascular dysfunction in the offspring. To this end, we
164 have utilised a rodent model of prenatal hypoxia developed by the Giussani laboratory

165 that does not affect maternal food intake, thereby allowing the effects of developmental
166 hypoxia to be studied in isolation ^{8,25-27}.

167

168 *2.2. Oxygen incubation protocols*

169 All procedures comply with The UK Animals (Scientific Procedures) Act 1986 and EU
170 directive 2010/63. The ARRIVE guidelines were followed for reporting the use of animals
171 in scientific experiments. Local ethical approval was granted by The University of
172 Manchester Animal Welfare Ethical and Review Board. Pregnant C57BL/J6 mice (aged
173 12 weeks, 24.1 ± 6.0 g), were bred, mated and maintained at The University of
174 Manchester (UK). Mice were housed in standard Individually Ventilated Cages (IVC)
175 with normal oxygen levels and a 12:12 light cycle with ad libitum food and water. The
176 pregnant mice were randomly assigned to two groups; normoxia (N, 21% O₂) or hypoxia
177 (H, 14% O₂). For hypoxic incubations, mice were transferred to an environmental
178 chamber (Coy O₂ In Vivo Glove Box, Coy Laboratory Products, Grass Lake, MI) at
179 gestational day (GD) 6 where they were subjected to 14% oxygen. Levels of humidity
180 (60%), CO₂ (<1%) and temperature (22°C) were controlled throughout chamber
181 incubation. Maternal food intake and water intake was monitored at regular intervals
182 throughout the procedure, and maternal body weight was measured before and after
183 chamber incubation. Mice were removed from the chamber at GD 18 and allowed to
184 litter in normoxia (GD 21 \pm 1 day). Litters were culled down to six (3 males and 3
185 females) to assure standardized maternal care and feeding. Sexing was done by visual
186 determination of the presence or absence of dark pigmentation on the perineum ^{28,29}.
187 Offspring were weaned from the mother at 3 weeks of age, and group housed in normal
188 conditions. Experiments were performed on mouse offspring aged between 25-32
189 weeks.

190

191

192 *2.3. Electron microscopy*

193 We used electron microscopy to assess left ventricular mitochondrial morphology in
194 adult mice aged between 30-32 weeks. 5 images were analyzed from each animal (n = 2
195 males and 2 females from normoxic pregnancies, and n = 5 males and 5 females from
196 hypoxic pregnancies). In brief, hearts were removed from the animal, the atria were
197 discarded, and the ventricles were cut longitudinally to separate the left and right
198 chambers. A section of the left ventricular free wall was isolated and 2mm horizontal
199 slices were taken from the mid myocardial layer; care was taken to isolate the same
200 area from each animal. The slices were immediately fixed by immersion with 4%
201 formaldehyde and 2.5% glutaraldehyde in 0.1M HEPES. The tissue was then removed
202 from the fixation solution and prepared according to the Elisman protocol ³⁰. Briefly, the
203 tissue was stained with heavy metals, dehydrated (stepwise), infiltrated with Taab 812
204 Hard Resin (stepwise), embedded in silicon wells and finally polymerized at 60°C for 24
205 hours ³¹. A single block was randomly selected from a bag and muscle orientation was
206 determined in semithin sections. Ultrathin sections (up to 1mm², Reichert Ultracut
207 ultramicrotome) were cut longitudinally in relation to the muscle fibres. Samples were
208 then attached to 200 mesh copper EM grids and imaged at x890 magnification with a
209 FEI Tecnai 12 Biotwin microscope at 80kV acceleration voltage with a Gatan Orius
210 SC1000 CCD camera. A grid was randomly selected, and squares were given
211 numerical values. A random number generator was used to select 5 grid squares per
212 animal and the images were analyzed using the free hand tool in Image J (version 1.52k,
213 National Institute of Health, MD). Mitochondria were traced and total mitochondrial area
214 was expressed relative to the total area of the cell (students were blinded to the
215 experimental sample).

216

217 *2.4. Mitochondrial function*

218 Mitochondrial function was investigated in male (n = 7 normoxic and 9 hypoxic) and
219 female (n = 7 normoxic and 8 hypoxic) offspring aged between 26-31 weeks.

220

221 *2.4.1. Mitochondrial oxygen consumption and H₂O₂ production*

222 Mitochondrial respiration was assessed by high-resolution respirometry using an
223 Oroboros Oxygraph-2k (Oroboros Instruments, Innsbruck, Austria) coupled to a
224 fluorescent LED2-Module, allowing simultaneous measurement of O₂ consumption and
225 H₂O₂ production, respectively. Mice were killed by cervical dislocation and the heart was
226 immediately excised. ~50mg of fresh left ventricular tissue was homogenized (IKA Ultra-
227 turrax T25) in mitochondrial respiration media (MiR05; containing: EGTA 0.5mM, MgCl₂
228 3mM, K-MES 60mM, KH₂PO₄ 10mM, HEPES 20mM, sucrose 110mM and 1% BSA).
229 0.16 ± 0.04 mg of homogenised tissue was injected into each of the two chambers of the
230 Oxygraph-2K for measurement of mitochondrial respiration and H₂O₂ production. The
231 rest of the homogenate was frozen at -80°C for analysis of enzymatic function (see
232 section 2.4.2). To measure H₂O₂ production, 10µM Amplex® UltraRed and 1U/ml
233 horseradish peroxidase (HRP) were added to each chamber. Amplex® UltraRed
234 oxidizes in the presence of H₂O₂ and forms resorufin, using HRP as a catalyst. Amplex®
235 UltraRed was excited at 563nm and emission was read at 587nm. 5U/ml superoxide
236 dismutase (SOD) was also added to the chambers to convert any extramitochondrial
237 superoxide (O₂⁻) to H₂O₂.

238

239 Substrate inhibitor titration protocols (SUIT protocols) were designed according to Pesta
240 et al ³² (see Fig. 1). Firstly, pyruvate (5mM), malate (2 mM) and glutamate (10mM) were
241 added to achieve LEAK respiratory state with complex I (CI) substrates in the absence of

242 adenylates (LEAK_{CI}). When oxygen consumption was stable, saturating ADP (5mM) was
243 injected to activate oxidative phosphorylation with CI substrates (OXPHOS_{CI}). Succinate
244 (10mM) was then added to assess the additive effects of complex II (CII) substrates on
245 oxidative phosphorylation (OXPHOS_{CI+CII}).

246

247

248

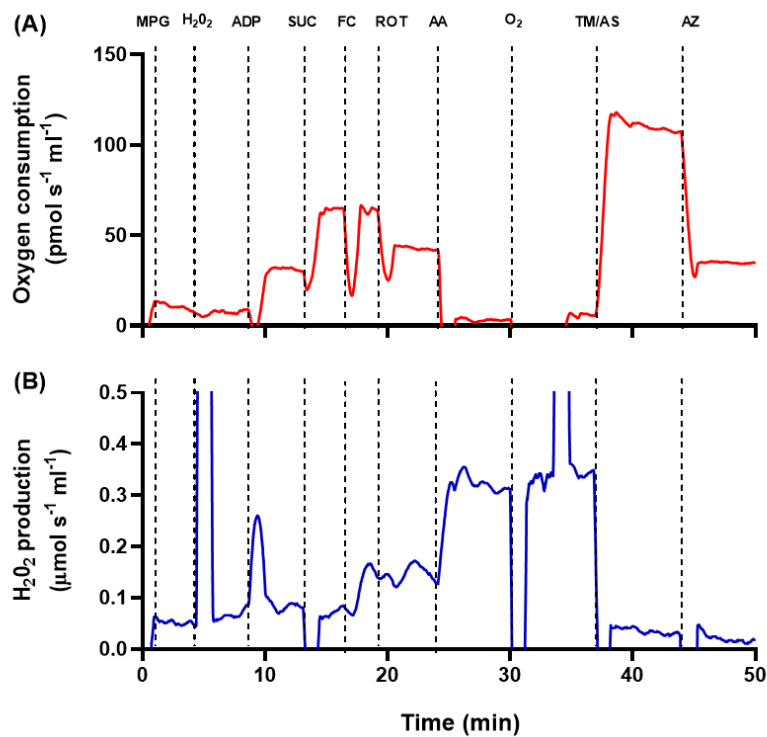
249

250

251

252

253



254

255 **Figure 1: Original trace of simultaneous measurement of mitochondrial**
256 **oxygen consumption and H₂O₂ production in mouse ventricular homogenate.**

257 Data is from a male offspring from a hypoxic pregnancy. Ventricular homogenate
258 (0.1 mg ml⁻¹) was added to the chamber and a range of substrates and inhibitors
259 were injected to investigate the electron transport chain (see methods section for
260 details). Abbreviations; MPG, malate pyruvate and glutamate; ADP, adenosine
261 diphosphate; SUC, succinate; FC, Carbonyl cyanide-4-
262 (trifluoromethoxy)phenylhydrazone (FCCP); ROT, rotenone; AA, antimycin-A; O₂,
263
264
265
266
267

268 *the chamber was opened for reoxygenation; TM/AS, N,N,N,N-tetramethyl-p-*
269 *phenylenediamine (TMPD) and ascorbate; AZ, azide.*

270

271 To uncouple mitochondria and assess maximum electron transfer capacity with CI+CII
272 substrates (ET_{CI+CII}), carbonyl cyanide-4-(trifluoromethoxy)phenylhydrazone (FCCP) was
273 titrated in steps to a final concentration of 0.1-0.3µM. Next, the CI inhibitor rotenone
274 (0.5µM) was added to assess ET_{CI+CII} with CII substrates only. To block the ET-pathway
275 and assess residual non-mitochondrial oxygen consumption (ROX), the complex III (CIII)
276 inhibitor, antimycin A, was added (2.5 µM). To assess complex IV (CIV) activity in
277 isolation, the electron donor N,N,N',N'-tetramethyl-p-phenylenediamine (TMPD, 0.5 mM)
278 was added in combination with ascorbate (2mM) to avoid autooxidation of TMPD.
279 Lastly, the CIV inhibitor sodium azide (50mM) was added to assess background non-
280 mitochondrial oxygen consumption from the addition of TMPD.

281

282 A separate protocol was used to assess the impact of CIV inhibition on H₂O₂ production
283 in control adult mice (n = 4). Ventricular homogenates were incubated with substrates to
284 achieve a steady-state OXPHOS_{CI+CII} (pyruvate, malate, glutamate, succinate and ADP)
285 whilst measuring H₂O₂ (HRP, amplex red and SOD). Next, sodium azide was titrated in
286 0.25mM steps from 0 to 1.75 mM to selectively inhibit CIV.

287

288 All O₂ consumption and H₂O₂ production data were normalized to a marker of
289 mitochondrial density, citrate synthase (CS) activity. When analyzing the effect of
290 sodium azide on H₂O₂ production, H₂O₂ was expressed as a percentage of the amount of
291 O₂ consumed (H₂O₂/O₂). To estimate mitochondrial efficiency of ATP production, the
292 OXPHOS-coupling efficiency ratio was calculated as 1 – (LEAK_{CI} / OXPHOS_{CI}), and the
293 respiratory control ratio (RCR) was calculated as OXPHOS_{CI} / LEAK_{CI})³³.

294

295 2.4.2. *Spectrophotometric analysis of enzymatic activities and antioxidant capacity*

296 Spectrophotometric assays were undertaken on ventricular homogenates from male (n =
297 5 normoxic and 5 hypoxic) and female (n = 6 normoxic and 6 hypoxic) frozen tissue
298 samples from (aged between 25-29 weeks). Homogenates were assayed for protein
299 content, citrate synthase activity and enzymatic activity of electron transport chain
300 complexes. For all assays, absorbance was measured with a BioTek Synergy HTX
301 multimode reader (BioTek, Swindon, UK). For enzymatic assays, values are expressed
302 as maximum enzymatic activity per min divided by protein content. Protein content of
303 ventricular homogenates were assessed using the Quick start Bradford dye reagent kit
304 (Bio-Rad laboratories, Watford, UK); absorption was read at 550nm at 25°C.

305

306 Protocols for measuring CI, CII and CIV enzyme activities, as well as citrate synthase
307 activity, were designed according to Spinazzi et al.³⁴. In brief, approximately 20-50mg of
308 frozen ventricular tissue was homogenized using a FastPrep-24™ 5G instrument (MP
309 Biomedicals, Santa Ana, CA) in solution containing 20mM TRIZMA-base, 40mM KCl,
310 2mM EGTA and 250mM Sucrose (pH 7.4). The tissue was homogenized in two cycles of
311 30 seconds with a 180-second pause in between each trial at 4°C. Samples were then
312 spun at 600g for 10 minutes at 4°C and the supernatant was stored in -80°C until the
313 day of the assay. Maximal enzymatic activity rate (V_{max}) was assessed over a ten-minute
314 period with a BioTek Synergy HTX multimode reader (BioTek, Swindon, UK) at 37°C.
315 The buffer components for each individual assay are given in Supplementary Table S1.

316

317

318 *2.5. Mitochondrial protein expression of electron transfer chain complexes*

319 Protein expression of complexes in the electron transport chain was measured with
320 Western Blot in males from normoxic (n = 5) and hypoxic (n = 5) pregnancies, and
321 females from normoxic (n = 5) and hypoxic (n = 5) pregnancies, aged between 26-32
322 weeks. The protocols have been described previously in detail ³⁵⁻³⁷. Following cardiac
323 excision, a ~0.5 cm³ region of the left ventricular free wall was removed, snap frozen and
324 stored in liquid nitrogen until analysis. Whole homogenates (~50 mg starting material)
325 were prepared in RIPA buffer with protease and phosphatase inhibitors (0.1mg/ml
326 phenylmethanesulphonylfuroide, 100 mmol/l sodium orthovanadate, 1 mg/ml aprotonin,
327 1 mg/ml leupeptin) and protein content was determined (DC Protein Assay, BioRad,
328 UK). Proteins were separated by PAGE and transferred to nitrocellulose membranes.
329 10µg of protein was used for each sample, and membranes were blocked with 5% milk
330 in TBS-T and incubated with the primary antibody cocktail (Abcam-110413, Cambridge,
331 UK: 1:1000 concentration) and the secondary antibody IRDye® 800CW IgG_{2a}-Specific
332 (Licor, UK: 1:20000 concentration). Membranes were visualized by chemiluminescence
333 (Syngene, UK) or IR-Dye labeled secondary antibodies (Licor, UK). As the 'classical'
334 housekeeping proteins can prove problematic with experimental treatments we opted for
335 a total protein stain to normalize for sample loading, as suggested by Li et. Al., ³⁸, and an
336 internal control to normalize between gels. Total protein transferred to the membrane
337 was determined by REVERT total protein stain (Licor, UK). Blots were repeated in
338 triplicate on separate occasions and data was averaged.

339

340 The antibody generated five separate bands, one for each protein corresponding to the
341 five complexes of the ETC pathway (Fig. 1 supplementary material). The value for each
342 separate protein in each sample was divided by the total value for the total protein as
343 well as the internal control.

344

345 *2.6. Calculations and statistics*

346 Maternal BW, FI, WI are expressed as scatter plots (including all measured points) and
347 statistically compared by fitting linear regression curves to compare slopes. Offspring
348 BW is presented as scatter plots expressing means \pm SEM and compared with mixed-
349 effect analysis using maternal oxygen level as the random effect and the Tukey's
350 correction for multiple comparisons test. For CIV inhibition, a linear regression curve was
351 fitted to the data to assess if the slope was non-zero. For mitochondrial density where
352 multiple observations (n) have been obtained from the same animal (N), linear mixed
353 modeling (SPSS Statistics. IBM, USA) was performed thus accounting for the nested
354 (clustered) design of the experiment e.g. multiple observations from the same heart (with
355 treatment (hypoxic/normoxic), sex and animal as co-factors). All remaining data were
356 statistically analyzed using a 2-way analysis of covariance (ANCOVA), with sex and
357 intrauterine oxygen levels as independent variables, and age as a covariate (n-values
358 and p-values are given in the figure legends). For mitochondrial H₂O₂ production, data
359 were log-transformed to obtain a normal distribution prior to performing the ANCOVA.

360

361 **3.0. Results**

362 *3.1. Maternal and offspring biometry*

363 There were no differences in maternal body weight, water intake or food intake between
364 normoxic and hypoxic dams (Fig. 2A-C), confirming that any programmed effects in the
365 offspring are most likely due to hypoxia alone, rather than differences in maternal food
366 consumption. There were no differences in offspring body weight between hypoxic and
367 normoxic groups at any of the ages tested (Fig. 2D-E).

368

369
370
371
372
373
374
375
376
377
378
379
380
381
382
383
384
385
386
387

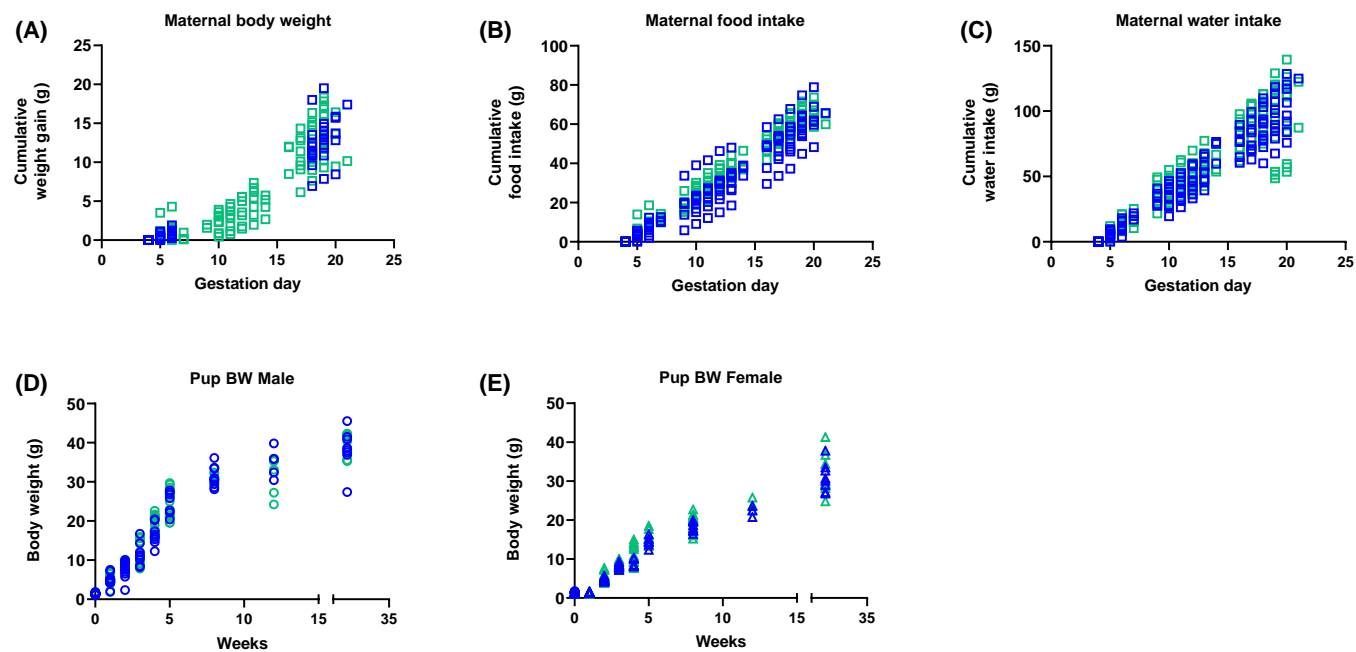


Figure 2: Effects of developmental hypoxia on maternal and fetal biometry. Maternal body weight (A), food (B) and water intake (C) were monitored in normoxic (green squares, $n = 16$) and hypoxic dams (blue squares, $n = 11$). Due to space restrictions within the environmental chamber, the body weight of pregnant dams could not be measured during the hypoxic incubation period (gestational days 6-18). Offspring body weight was also monitored in males (D, circles) from normoxic and hypoxic pregnancies ($n = 24$ offspring from 9 pregnancies and 23 offspring from 8 pregnancies, respectively) and females (E, triangles) from normoxic and hypoxic pregnancies ($n = 20$ offspring from 8 pregnancies and 20 offspring from 7 pregnancies, respectively) from birth to 15 weeks. Data are presented as scatter points for measurements of an individual animal. Statistics were run using a mixed-model effects with Tukey's correction for multiple comparisons.

388 3.2. *Offspring mitochondrial oxygen consumption*

389 Mitochondrial homogenate preparations were of good quality, as attested by high
390 respiratory control ratios (9.2 +/- 0.3) and OXPHOS-coupling efficiency ratios (0.89 +/-
391 0.006) with complex I substrates (malate, pyruvate and glutamate). Mitochondrial
392 oxygen consumption and H₂O₂ production responded to substrates and inhibitors in the
393 expected manner³⁹ (Fig. 1), but FCCP had modest effects on mitochondrial respiration
394 with only 9.3% of preparations responding positively. In the other preparations, even
395 very low concentrations of FCCP (<0.1 μM) had no effect on oxygen consumption or
396 caused a small inhibition (see Fig. 1A), suggesting that mouse cardiac homogenates are
397 already operating at or near their theoretical maximum rate of oxygen consumption.

398

399 In male mice, developmental hypoxia reduced mitochondrial oxygen consumption in the
400 Leak_{CI} and OXPHOS_{CI} states, as well as flux through CIV alone (Fig. 3, circular
401 symbols). In contrast, developmental hypoxia increased mitochondrial oxygen
402 consumption in female mice in all states, except for LEAK_{CI} (Fig. 3, triangular symbols).
403 Within the normoxic group, male mitochondrial oxygen consumption was higher than
404 females in all respiratory states (Fig. 3, green symbols), but there were no sex-
405 dependent differences in the hypoxic group (Fig. 3, blue symbols). There was no effect
406 of treatment or gender on the OXPHOS-coupling efficiency ratio (Fig. 3F) or the RCR
407 (data not shown).

408

409

410

411

412

413

414

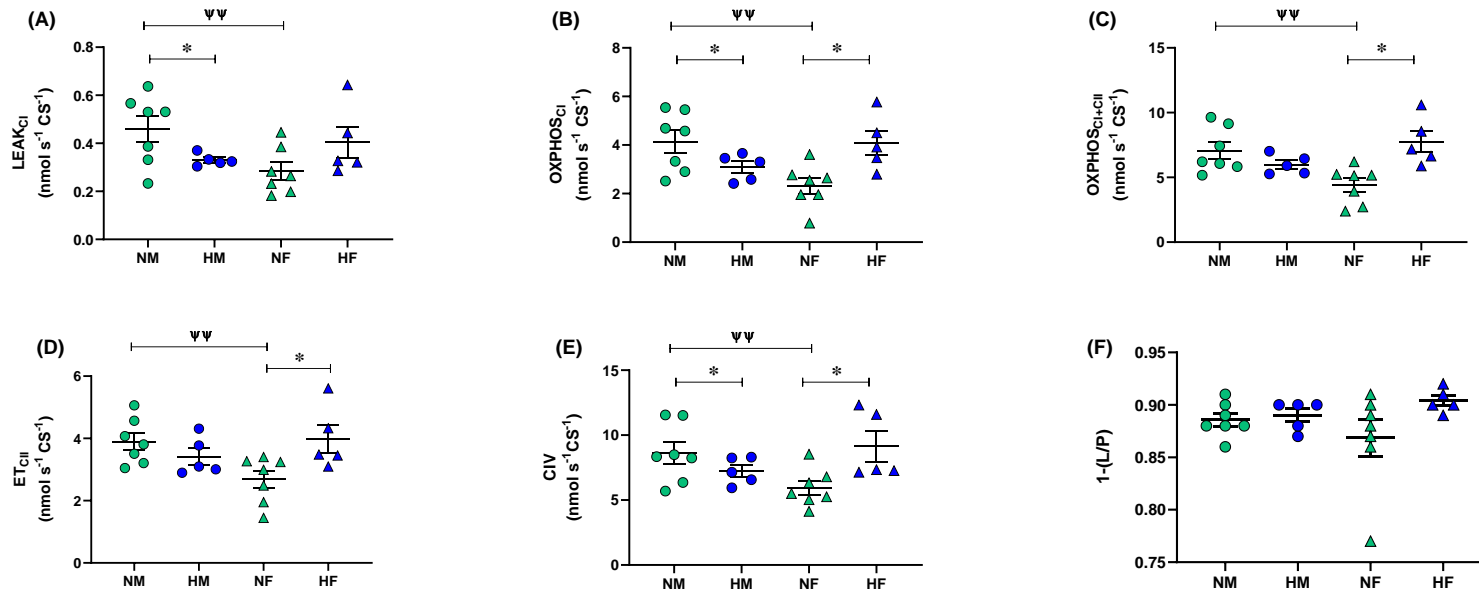
415

416

417

418

419



420 **Figure 3: Effect of developmental hypoxia on mitochondrial oxygen consumption.** Mitochondrial oxygen consumption was
421 measured in males from normoxic (green circles, $n = 6-7$) and hypoxic (blue circles, $n = 8-9$) pregnancies, and females from
422 normoxic (green triangles, $n = 7$) and hypoxic (blue triangles, $n = 8$) pregnancies. Each panel represents a different respiratory state;
423 (A) Leak respiration with substrates for complex I (LEAK_{CI}), (B) oxidative phosphorylation with substrates for complex I (OXPHOS_{CI}),
424 (C) oxidative phosphorylation with substrates for Complex I and II (OXPHOS_{CI+CIII}), (D) electron transfer capacity with substrates for
425 Complex II (ET_{CIII}), (E) electron donation to Complex IV (CIV) and (F) OXPHOS-coupling efficiency ratios (1-(L/P)). Data are mean \pm
426 SEM. Asterisk denotes a difference between mice from normoxic and hypoxic pregnancies, and Ψ denotes a difference between
427 male and female mice (Two-way ANCOVA, one symbol = $p < 0.05$, two symbols = $p < 0.01$).

428 3.3. *Offspring mitochondrial H₂O₂ production*

429 In male mice, developmental hypoxia increased H₂O₂ production when it was measured
430 in the LEAK_{CI} state and when CIII was inhibited with antimycin A (Fig. 4A and F, circular
431 symbols). In contrast, females from hypoxic pregnancies produced less H₂O₂ compared
432 to their normoxic counterparts in the OXPHOS_{CI+CII} state, and in the ET states (Fig. 4,
433 triangular symbols). With regard to sex-dependent differences, normoxic male H₂O₂
434 production was higher than normoxic females in all respiratory states (Fig. 4, green
435 symbols), but there were no differences in H₂O₂ production between hypoxic males and
436 hypoxic females (Fig. 4, blue symbols).

437

438 Having discovered differences in mitochondrial oxygen consumption and H₂O₂ production
439 between treatment groups, we next sought to determine the underlying mechanisms. In
440 principle, changes in CIV oxygen consumption (Fig. 3E) may account for differences in
441 basal H₂O₂ production between experimental groups. To explore this possibility, we
442 performed experiments in control adult mice where we partially inhibited CIV with sodium
443 azide and simultaneously measured H₂O₂ production (Fig. 5). We found that a dose-
444 dependent inhibition of CIV caused a stepwise increase in H₂O₂ production.

445

446

447

448

449

450

451

452

453

454

455

456

457

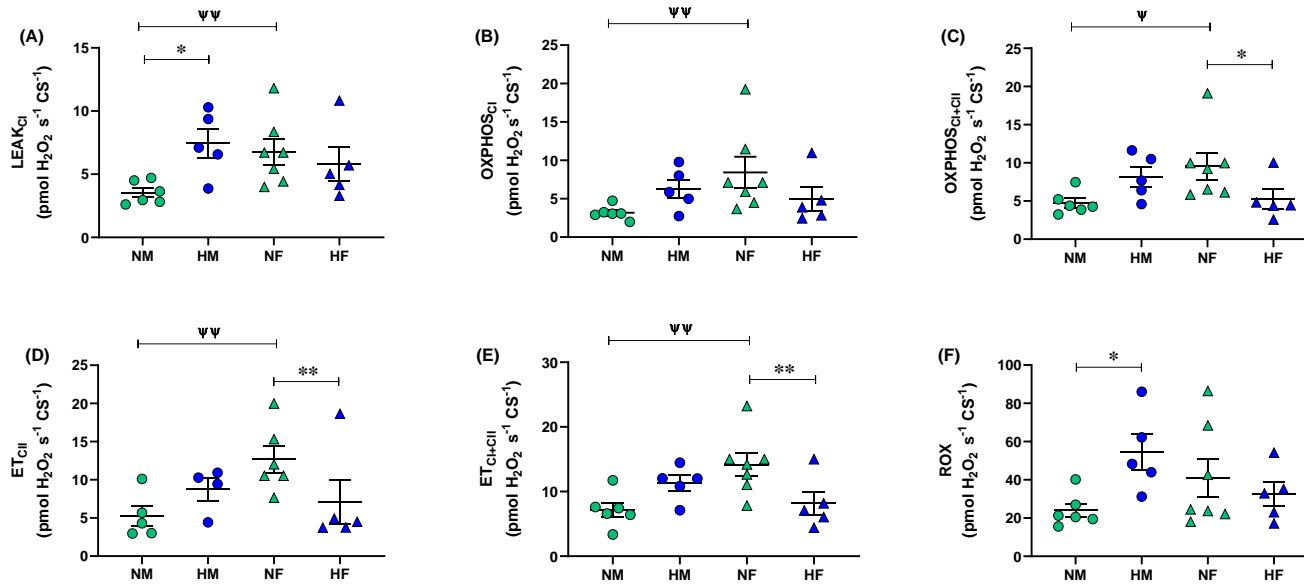
458

459

460

461

462



463 **Figure 4: Effects of developmental hypoxia on mitochondrial H₂O₂ production.** H₂O₂ production was measured in males from
464 normoxic (green circles, n = 5) and hypoxic (blue circles, n = 5) pregnancies, and females from normoxic (green triangles, n = 5) and
465 hypoxic (blue triangles, n = 6) pregnancies. Each panel represents a different respiratory state; (A) Leak respiration with substrates
466 for complex I (LEAK_{CI}), (B) oxidative phosphorylation with substrates for complex I (OXPHOS_{CI}), (C) oxidative phosphorylation with
467 substrates for complex I and II (OXPHOS_{CI+CI}), (D) electron transfer capacity with substrates for complex II (ET_{CI}), (E) electron
468 transfer capacity with substrates for complex I+II (ET_{CI+CI}), and (F) residual oxygen consumption (ROX) in the presence of antimycin
469 A. Data are mean ± SEM. Asterisk denotes a statistically significant difference between mice from normoxic and hypoxic
470 pregnancies, and Ψ denotes a difference between male and female mice (Two-way ANCOVA, one symbol = p < 0.05, two symbols =
471 p < 0.01).

472
473
474
475
476
477
478
479
480
481
482
483
484
485
486
487
488
489
490
491
492
493
494
495
496
497
498
499
500
501
502
503
504
505

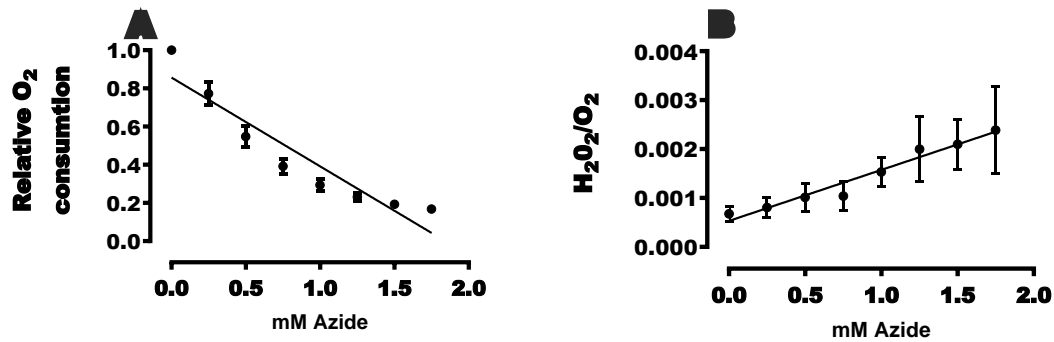


Figure 5: Relationship between complex IV activity and H₂O₂ production. Oxygen consumption (A) was measured simultaneously with H₂O₂ production (B) during dose-dependent inhibition of complex IV with sodium azide. Data are presented as mean \pm SEM, n=4 adult females from normoxic pregnancies in both panels. A linear regression curve was fitted to the data and was found to be significantly different from zero.

3.4. Offspring mitochondrial morphology

Differences in mitochondrial oxygen consumption and H₂O₂ production between experimental groups may also be explained by variable mitochondrial densities. Therefore, we investigated mitochondrial morphology with electron microscopy and measured the enzymatic activity of a common marker for mitochondrial content, citrate synthase. Developmental hypoxia had no effect on mitochondrial density or citrate synthase activity in any of the treatment groups (Fig. 6) and there were no differences between genders.

506
 507
 508
 509
 510
 511
 512
 513
 514
 515
 516
 517
 518
 519
 520
 521
 522
 523
 524
 525
 526
 527
 528
 529
 530
 531
 532
 533
 534
 535

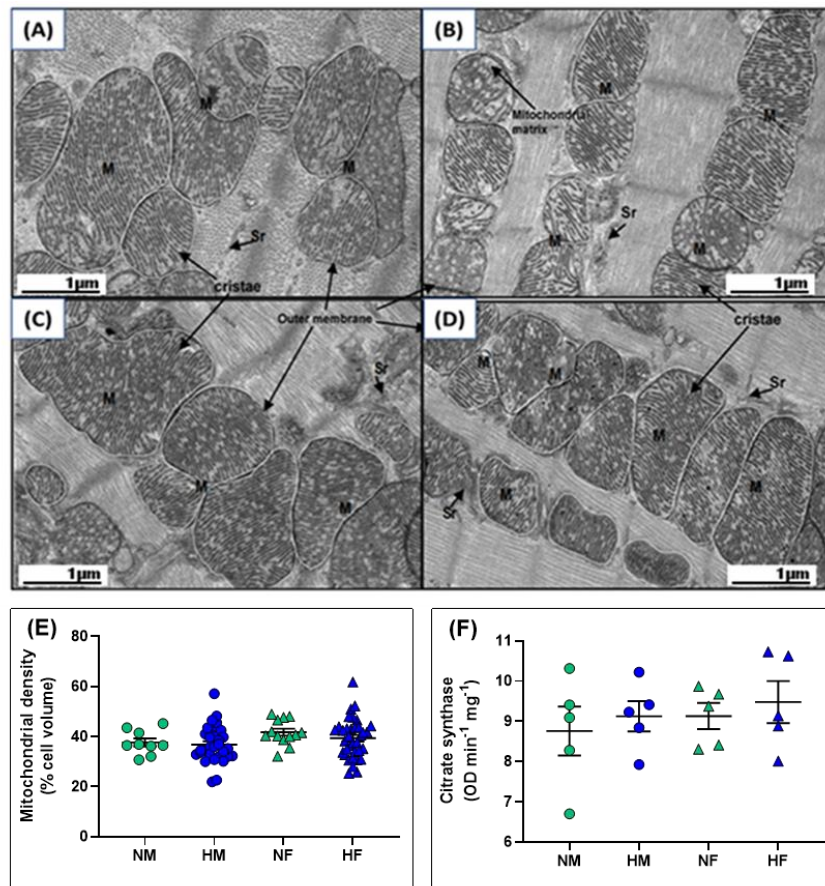


Figure 6: Effects of developmental hypoxia on mitochondrial density and citrate synthase activity. Transmission electron microscope images of left ventricular mitochondria in male offspring from normoxic (A, N = 2) and hypoxic (B, N = 5) pregnancies, and female offspring from normoxic (C, N = 2) and hypoxic (D, N = 5) pregnancies. Labels in image represent; M: mitochondria; Sr: sarcoplasmic reticulum; Scale bar: 1 μM. Panel E-F show mean data ± SEM for mitochondrial density (n = 5 images per mouse) and citrate synthase activity (n = 5 offspring per group), respectively. For mitochondrial density, linear mixed modeling was performed to account for the nested (clustered) design of the experiment e.g. multiple observations from the same animal. For citrate synthase activity, a 2-way ANCOVA was performed. No statistical differences were found between any of the experimental groups.

536 3.5. Offspring mitochondrial enzymatic activity

537 Next, we investigated the possibility that differences in mitochondrial oxygen
538 consumption and H₂O₂ production were underlined by variable enzymatic activities of
539 complexes in the electron transport chain. We found that male offspring from hypoxic
540 pregnancies had higher CI enzymatic activity (Fig. 7A), compared to their normoxic
541 counterparts, and females from hypoxic pregnancies had lower CII activity (Fig. 7B) and
542 higher CIV activity (Fig. 7C), compared to their normoxic counterparts.

543

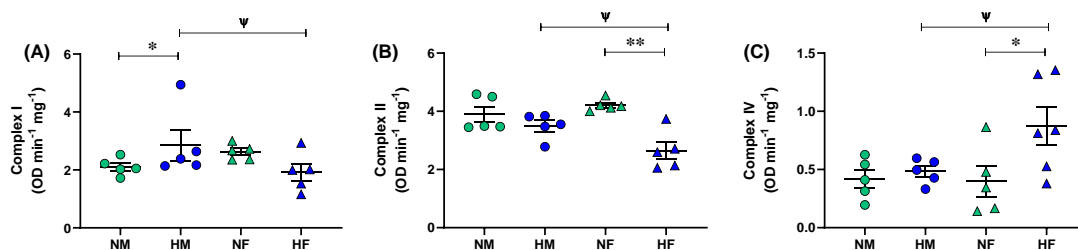
544

545

546

547

548



549 **Figure 7: Effects of developmental hypoxia on the activity of key**
550 **mitochondrial enzymes.** Enzymatic activity of complex I (A), complex II (B) and
551 complex IV (C) were measured in males from normoxic (green circles, n = 5) and
552 hypoxic (blue circles, n = 5) pregnancies, and females from normoxic (green
553 triangles, n = 5) and hypoxic (blue triangles, n = 6) pregnancies. Data are
554 presented as mean ± SEM. Asterisk signifies a statistically significant difference
555 between mice from normoxic and hypoxic pregnancies (Two-way ANCOVA, one
556 symbol = p < 0.05, two symbols = p < 0.01).

557

558 With regards to gender-specific effects, there were no differences in enzymatic activity
559 between males and females in offspring from normoxic pregnancies, but females from
560 hypoxic pregnancies had lower CI and CII activity, and higher CIV activity, compared to
561 their male counterparts (Fig. 7A-C).

562

563

564 3.6. *Offspring mitochondrial complex I-V protein expression*

565 Lastly, we investigated the possibility that differences we observed in mitochondrial
566 function could be explained by differential protein expression of electron transport chain
567 complexes. CI, CII and CIV protein expression were lower in males from hypoxic
568 pregnancies, compared to their normoxic counterparts (Fig. 8A, B and D), but there were
569 no differences in the female group. Within the normoxic group, males had higher CI, CII
570 and CIV protein expression compared to females (Fig. 8A, B and D), but there were no
571 sex-specific effects within the hypoxic group.

572

573

574

575

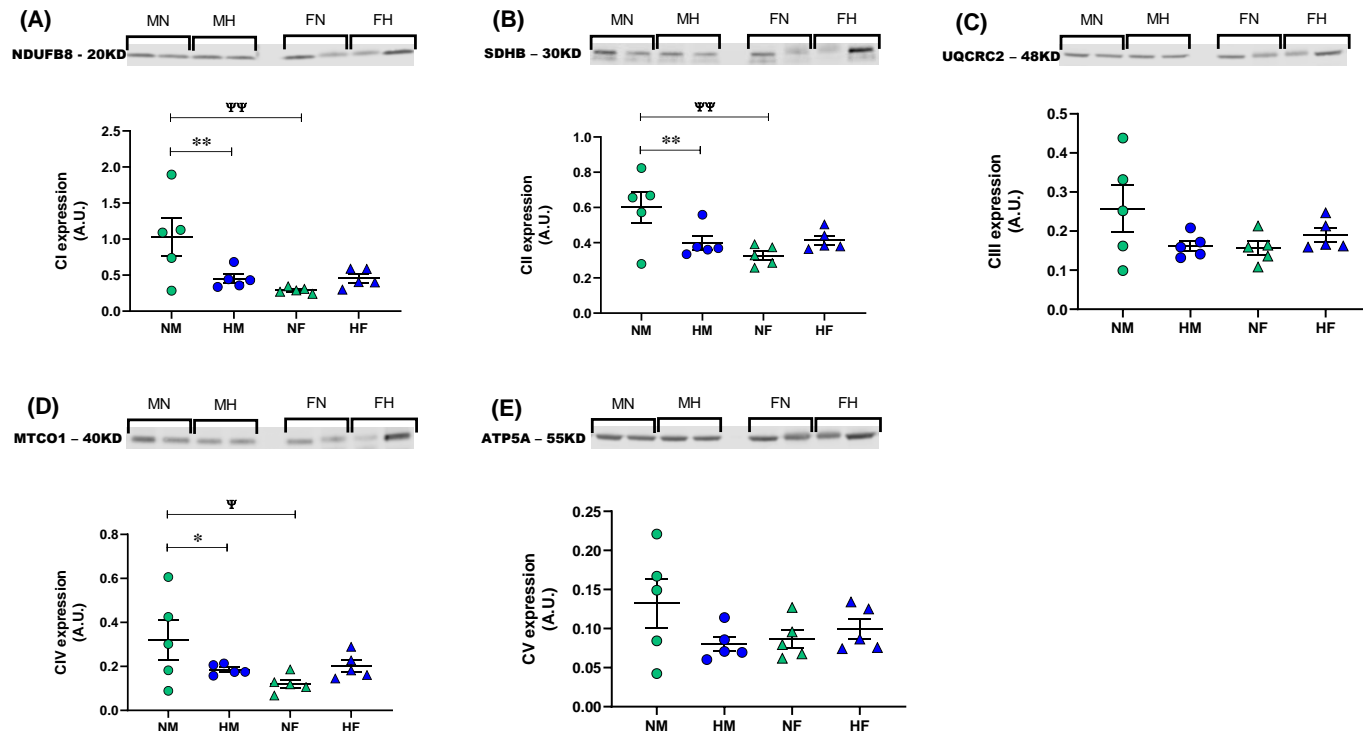
576

577

578

579

580
581
582
583
584
585
586
587
588
589
590
591



592 **Figure 8: Effect of developmental hypoxia on protein expression of respiratory chain Complexes.** Protein expression was
593 measured with Western Blot in males from normoxic (green circles, $n = 5$) and hypoxic (blue circles, $n = 5$) pregnancies, and females
594 from normoxic (green triangles, $n = 5$) and hypoxic (blue triangles, $n = 6$) pregnancies. Each panel represents a different complex in
595 the respiratory chain; complex I (A), II (B), III (C), IV (D) and V (E). Data are mean \pm SEM. Asterisk denotes a difference between
596 mice from normoxic and hypoxic pregnancies, and Ψ denotes a statistically significant difference between male and female mice
597 (Two-way ANCOVA, one symbol = $p < 0.05$, two symbols = $p < 0.01$). The full Blot is given in supplementary Figure S1.

598 **4.0. Discussion**

599 This is the first comprehensive study to address the effects of developmental hypoxia on
600 mitochondrial function in adult offspring. We show that male adult offspring from hypoxic
601 pregnancies possess mitochondria with a reduced respiratory capacity, increased H₂O₂
602 production and a lower protein expression of CI, CII and CIV. In contrast, females from
603 hypoxic pregnancies had a higher respiratory capacity, greater CIV enzymatic activity,
604 and reduced H₂O₂ production, despite lower enzymatic activity of CII. From these results,
605 we speculate that early exposure to hypoxia has long term sex-dependent effects on
606 metabolic function, which may have implications for susceptibility to cardiac disease in
607 adulthood.

608

609 *4.2. Effects of developmental hypoxia on male offspring mitochondrial function*

610 The first major and novel finding from this study is that male offspring from hypoxic
611 pregnancies had greater levels of basal H₂O₂ production, compared to their normoxic
612 counterparts. Previous studies have shown developmental hypoxia can cause oxidative
613 stress in fetal ²² and perinatal ⁴⁰ mammals, but to our knowledge, this is the first study to
614 show developmental hypoxia can programme ROS levels in adulthood. It is well-known
615 that the over-production of mitochondrial ROS plays a major role in cardiac pathologies,
616 particularly I/R injury ⁴¹. Interestingly, several studies have shown developmental
617 hypoxia programmes cardiac sensitivity to I/R injury in adult male offspring ^{7,11,12}, partly
618 due to the downregulation of protein kinase C epsilon (PKCε) via DNA methylation ¹³. In
619 addition to differential expression of PKCε, it is tempting to speculate that elevated basal
620 H₂O₂ production sets a functional deficit in the hearts of males from hypoxic pregnancies,
621 which may predispose them to postischemic oxidative stress.

622

623 Our data provides some information on the possible mechanism underlying the elevated
624 basal H₂O₂ production in males from hypoxic pregnancies. H₂O₂ production in hypoxic
625 males was higher than their normoxic counterparts in all respiratory states (although it
626 only reached statistical significance in the LEAK_{Cl} state), and the difference was also
627 apparent in the presence of rotenone and antimycin A, which block the CI_Q and CIII_Q
628 ROS sites, respectively ⁴². In the presence of these inhibitors, ROS production
629 commonly occurs at the CIII_Q site, which is a major source of oxidative stress in the
630 postischemic heart ⁴³. Nevertheless, pharmacological inhibition of the CIII_Q site (e.g.
631 with myxothiazol or stigmatellin) would be necessary to confirm its involvement because
632 other sites proximal to CIII can contribute to ROS production under these conditions ⁴².
633 Furthermore, other factors may explain our results, including differential antioxidant
634 profiles. Clearly, further research is necessary to confirm the site or source of elevated
635 H₂O₂ production in males from hypoxic pregnancies.

636

637 In addition to H₂O₂ production, developmental hypoxia significantly reduced mitochondrial
638 oxygen consumption in LEAK_{Cl} and OXPHOS_{Cl} states, as well as flux through CIV alone.
639 The reduction in mitochondrial respiration was associated with a decrease in CI, CII and
640 CIV protein expression, suggesting that these complexes are downregulated by
641 developmental hypoxia, leading to lower respiratory capacity. These results are in
642 agreement with data from Thompson's group ^{19,20} that showed developmental hypoxia
643 reduces mitochondrial respiration rate and enzymatic activities of CI and CIV in adult
644 male guinea pigs from hypoxic pregnancies. A reduction in mitochondrial respiratory
645 capacity compromises ATP production, especially under situations of increased
646 metabolic demand, such as exercise or disease. Therefore, in addition to elevated basal

647 H₂O₂ production, limitations in mitochondrial electron transport may contribute to cardiac
648 dysfunction and sensitivity to I/R in males from hypoxic pregnancies.

649

650 The mitochondrial phenotype in males from hypoxic pregnancies may be explained by
651 several factors. It is possible that developmental hypoxia directly altered fetal
652 mitochondrial function and the phenotype persisted into adulthood. Indeed, several
653 studies have shown intrauterine stress alters embryonic and fetal mitochondria, leading
654 to the overproduction of ROS and a self-reinforcing cycle of mitochondrial dysfunction
655 that persists into adulthood, and may even be inherited ^{44,45}. In support of this idea, a
656 previous study found evidence of oxidative stress in male fetal guinea pig hearts
657 exposed to 10.5% oxygen, and this was associated with a reduction in the enzymatic
658 activity of CIV ²². Alternatively, developmental hypoxia may have altered fetal
659 mitochondria indirectly due to its effects on cardiac structure. The foetus initially
660 responds to hypoxia by preferentially distributing blood flow to the heart and brain, which
661 eventually leads to increased peripheral resistance and cardiac remodeling ⁴⁻⁶. This
662 remodeling is apparent at the cellular level ⁴⁶⁻⁴⁸, which may require mitochondrial
663 alterations. Lastly, mitochondrial programming by intrauterine stress could also be
664 achieved via stable epigenetic alterations to the nuclear genome ⁴⁹. Indeed, recent
665 studies have shown developmental hypoxia alters global DNA methylation patterns in
666 rats leading to a reprogramming of the cardiac transcriptome, with a major focus on
667 mitochondrial genes ⁵⁰. Therefore, the observed differences in male mitochondrial
668 protein expression in the present study may have epigenetic origins. Integrative
669 longitudinal studies that monitor the effects of developmental hypoxia on mitochondrial
670 function across the life course would help to discern between these possibilities.

671

672 4.2. Effects of developmental hypoxia on female offspring mitochondrial function

673 The second major and novel finding from this study is that adult female offspring from
674 hypoxic pregnancies possess mitochondria with a higher respiratory capacity, increased
675 mitochondrial efficiency and lower levels of basal H₂O₂ production. These results
676 suggest developmental hypoxia programmes a mitochondrial phenotype in females that
677 can generate ATP at a higher capacity and efficiency, while limiting ROS production. To
678 our knowledge, this is the first study which has shown developmental hypoxia can
679 programme a seemingly advantageous metabolic phenotype. From this perspective, it is
680 interesting to note that several studies have shown female hearts are less affected by
681 developmental hypoxia than males ^{20,51,52}, and they also recover better from I/R injury
682 ^{7,11,12}. In theory, a greater mitochondrial respiratory capacity and lower H₂O₂ production
683 could help to sustain ATP production and limit oxidative stress during oxygen and/or
684 nutrient deprivation. Therefore, we propose that mitochondrial adaptations programmed
685 by developmental hypoxia may protect the female heart from subsequent I/R stress in
686 adulthood.

687

688 The increased respiratory capacity in females from hypoxic pregnancies was present
689 under all respiratory states (except for Leak respiration), and with substrate
690 combinations for CI and CII, as well as direct electron transfer to CIV with TMPD.
691 Therefore, one mechanistic explanation is that developmental hypoxia increased
692 mitochondrial density in female mice. However, analysis of cardiomyocyte EM images
693 found no significant differences in mitochondrial content between females from normoxic
694 or hypoxic pregnancies. While we acknowledge that our EM analysis has limitations and
695 a more robust approach should be taken to confirm these morphological findings (i.e.
696 using stereology or 3D reconstruction), we also found no differences in female citrate
697 synthase activity, which is an excellent marker of mitochondrial content⁵³. Taken
698 together, it seems unlikely that the differences in respiratory capacity between females

699 from normoxic and hypoxic pregnancies is related to mitochondrial content. An
700 alternative explanation is that developmental hypoxia increases CIV activity in female
701 mice. In support of this explanation, enzymatic activity of CIV was elevated in females
702 from hypoxic pregnancies, compared to their normoxic counterparts, and this was
703 associated with a trend towards higher CIV protein expression. In addition to increasing
704 respiratory capacity, enhanced complex IV activity is also known to increase
705 mitochondrial oxygen affinity which is beneficial for maintaining ATP production under
706 conditions of low oxygen availability, such as I/R injury ^{54,55}. Therefore, it would be
707 interesting to investigate the effects of developmental hypoxia on female mitochondrial
708 oxygen kinetics.

709

710 With regard to the mechanism underlying the reduced basal H₂O₂ production, enzymatic
711 activity and protein expression of the main ROS producing complexes (CI and CIII) were
712 not altered by developmental hypoxia in female mice. However, theoretically, the
713 increase in CIV activity in females from hypoxic pregnancies could decrease the
714 reduction of redox centers in CI or CIII, thereby reducing electron leak and ROS
715 generation from these complexes ⁵⁶. To explore this possibility, we performed
716 experiments in control adult mice where we partially inhibited CIV with sodium azide and
717 simultaneously measured H₂O₂ production. We found that a dose-dependent inhibition of
718 CIV caused a stepwise increase in H₂O₂ production. This relationship has been
719 demonstrated previously in isolated cardiomyocytes from embryonic chick
720 cardiomyocytes where reduced CIV leads to enhanced ROS production ⁵⁷. Therefore,
721 greater CIV activity in females from hypoxic pregnancies may contribute to the observed
722 reduction in H₂O₂ production in this experimental group. Nevertheless, there are other
723 mechanistic explanations to explore, including differences in antioxidant capacity.

724

725 The mechanisms underlying mitochondrial programming in female mice are likely to be
726 similar to males (discussed above), but the resultant phenotype is obviously very
727 different. These results are strongly aligned to numerous studies that have
728 demonstrated sex-dependent differences in the susceptibility of offspring to fetal stress
729 (reviewed in^{45,58,59}). Identifying the underlying cause of these differences is an active
730 area of research, but recent work suggests several fundamental differences between
731 males and females may influence programming susceptibility, including; pattern of
732 development (genetic, transcriptional and morphological), growth rate, sex hormones,
733 placental plasticity, the regulation of epigenetic processes, metabolic hormones, the rate
734 of ageing and lifespan^{45,58}. With regard to the cardiovascular system, several studies
735 have shown oestrogen plays a protective role in the programming of hypertension, while
736 testosterone is detrimental⁵⁹. Given that oestrogen is also known to modulate cardiac
737 mitochondrial biogenesis, oxidative phosphorylation and ROS production⁶⁰, this hormone
738 may have played a role in orchestrating the gender-specific responses in the present
739 study. In this respect, it would be interesting to repeat the experiment in ovariectomized
740 and castrated mice. There is also strong evidence that sex-dependent differences in
741 placental plasticity play a major role in cardiovascular programming ⁶¹. Indeed,
742 numerous studies have shown developmental hypoxia leads to placental remodeling in
743 rodents ⁶²⁻⁶⁵, with female placentas adapting much better than males ⁶⁶. Given the
744 essential role that the placenta plays in the provision of fetal nutrients, sex-dependent
745 placental remodeling may have important consequences for cardiac function and
746 metabolism. Lastly, recent work has shown that epigenetic and transcriptomic
747 signatures associated with developmental hypoxia are sex-dependent ⁶⁷, and
748 predominantly mitochondrial ⁵⁰. Therefore, the gender-specific mitochondrial protein
749 expression that we observed may represent persistent epigenetic marks.

750

751 4.3. Effects of gender on mitochondrial structure and function in offspring from normoxic
752 pregnancies

753 Previous work has demonstrated substantial differences between males and females in
754 mitochondrial structure and function, but the results are highly tissue-specific. In most
755 tissues, including liver, brain, adipose and skeletal muscle, females exhibit a higher
756 respiratory capacity than males, which is often associated with greater mitochondrial
757 content ⁶⁸. In contrast, two studies found no differences in cardiac mitochondrial
758 respiratory capacity between male and female rats, despite a reduced mitochondrial
759 content in females ^{69,70}. Furthermore, a third study found mitochondrial respiration with
760 glutamate and malate was higher in males compared to females ⁷¹. In line with this latter
761 study, we found male normoxic mice had a greater respiratory capacity than their female
762 counterparts, and this difference was present in all respiratory states and substrate
763 combinations, as well as CIV flux with TMPD. We go further to show the increase in
764 male respiratory capacity was associated with higher male CI, CII and CIV protein
765 expression, providing a mechanistic explanation for these sex-dependent differences.

766

767 In addition to respiratory capacity, previous work has shown sex-dependent differences
768 in cardiac ROS production. In general, female cardiomyocytes generate less ROS than
769 males at rest and after pathological stimuli, and they are also less prone to age-
770 dependent oxidative stress ^{69,72,73}. Some studies suggest the reduced ROS production
771 in females is due to a superior antioxidant capacity ⁷³, while others point towards
772 reduced electron leak from CI and CIII ⁶⁹. In contrast to these studies, normoxic males in
773 our study had lower basal H₂O₂ production than their female counterparts in all
774 respiratory states and substrate combinations. We cannot explain the discrepancy
775 between these studies, but factors such as species, strain and age may play a role in
776 determining sex-dependent differences.

777

778 **5.0. Conclusions and future directions**

779 In conclusion, our study has shown developmental hypoxia has long-term, sex-specific
780 implications for metabolism. We speculate that these differences may have implications
781 for disease susceptibility. For example, increased basal H₂O₂ production and lower
782 respiratory capacity in males from hypoxic pregnancies may predispose mitochondria to
783 cardiac dysfunction and I/R injury, a condition that is largely driven by oxidative stress⁴¹.
784 In contrast, the greater respiratory capacity and lower H₂O₂ production in females from
785 hypoxic pregnancies may help to sustain ATP production and limit oxidative stress under
786 conditions of oxygen deprivation. These sex-specific differences in response to
787 developmental hypoxia may help to explain why females from hypoxic pregnancies are
788 less susceptible to I/R injury, compared to their male counterparts^{11,12}. While purely
789 speculative at this stage, the present study provides the foundation to test this
790 hypothesis and design future gender-specific metabolic therapies to prevent cardiac
791 dysfunction in offspring from hypoxic pregnancies.

792

793 **6.0 Acknowledgements**

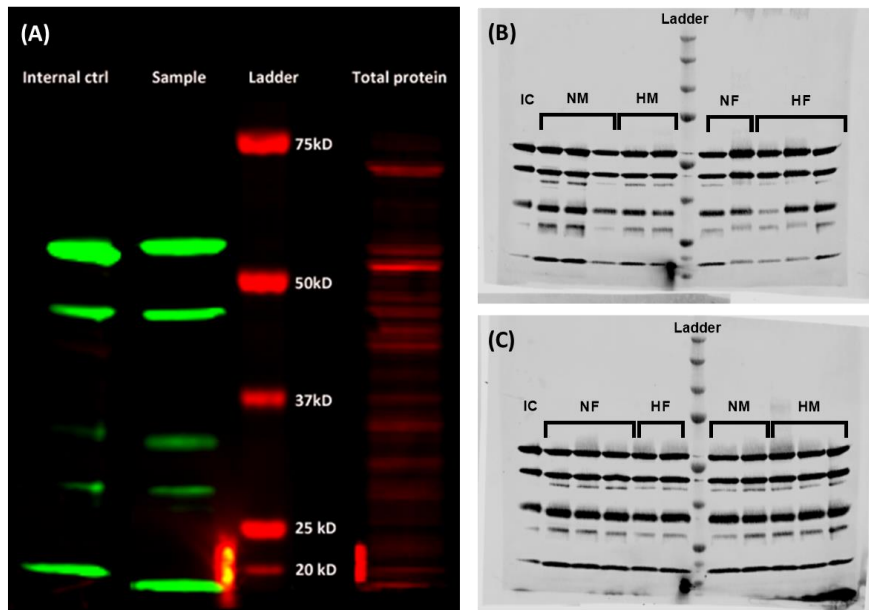
794 This study was funded by a PhD studentship awarded to Kim Hellgren by the Medical
795 Research Council Doctoral Training Partnerships. We would like to thank Aleksandr
796 Mironov, Dr. Christian Pinali and Samantha Forbes for their help in acquiring and
797 interpreting the EM images. In addition, we would like to thank Dr. Katherine Dibb, Dr
798 Javier Iglesias-Gonzalez and Professor David Eisner for their much-valued advice during
799 the study.

800 **Supplementary Tables and Figures**801 **Table S1: Conditions for spectrophotometric assays of respiratory chain enzymes and citrate synthase activities in**
802 **ventricular homogenates**

	CI	CII	CIV	CS
λ (nm)	600	600	550	412
Buffer	KP, 50mM	KP, 25 mM	KP, 50mM	TRIS, 100mM
pH	7.50	7.50	7.5	8.0
Substrates/electron acceptors	NADH 100 μM; DCPIP 80 μM; Ub-1 60 μM	Succinate 20 mM; DCPIP 80 μM; DUB 50 μM	Cyt c H ₂ ; 60 μM	DTNB 100 μM; Ac CoA 300 μM; Oxaloacetate 0.5mM
Other reagent(s)	BSA 3 mg ml ⁻¹ ; KCN 300 μM	BSA 1 mg ml ⁻¹ ; KCN 300 μM	KCN 300 μM	Triton X-100 0.1%;
Specific inhibitor	Rotenone 10 μM	Malonate 10 mM	KCN 300 μM	-

Abbreviations: CI, complex I; CII, complex II; CIV, complex IV; CS, citrate synthase; λ, selected wavelength for the assay; ε, extinction coefficient; Ac CoA, acetyl coenzyme A; BSA, fatty acid-free bovine serum albumin; Cyt c H₂, reduced cytochrome c; DCPIP, 2,6-dichlorophenolindophenol; DUB, decylubiquinol; DTNB, 5,5'-dithiobis(2-nitrobenzoic acid); KCN, potassium cyanide; KP, potassium phosphate buffer; Tris, Tris buffer; Ub1, ubiquinone 1

803
804
805
806
807
808
809
810
811
812



813 **Figure S1: Representative images of Western Blots for one replicate.** (A) Each gel was loaded and imaged at two wavelengths;
814 the samples and an internal control (historical left ventricular mouse sample that was used for all blots) were loaded with the antibody
815 and imaged at 800nm (green bands: top to bottom; complex V, complex III, complex IV, complex II, and complex I). In addition, a
816 ladder and the total protein stain, REVERT, was imaged on the same Blot at 700nm (red bands). (B-C) Original Blots for one
817 replicate showing sample protein expression of Complexes V, III, IV, II and I (top to bottom) in an internal control (IC), normoxic
818 female (NF, n = 5), hypoxic female (HF, n = 5), normoxic male (NM, n = 5) and hypoxic male (HM, n = 5). Averages for three
819 replicates are given in Figure 8 of the main manuscript.

820 **References**

821

- 822 1. Dagenais, G.R., *et al.* Variations in common diseases, hospital
823 admissions, and deaths in middle-aged adults in 21 countries from five
824 continents (PURE): a prospective cohort study. *The Lancet*.
- 825 2. Barker, D.J.P., Osmond, C., Winter, P.D., Margetts, B. & Simmonds, S.J.
826 WEIGHT IN INFANCY AND DEATH FROM ISCHAEMIC HEART
827 DISEASE. *The Lancet* **334**, 577-580 (1989).
- 828 3. Hutter, D., Kingdom, J. & Jaeggi, E. Causes and Mechanisms of
829 Intrauterine Hypoxia and Its Impact on the Fetal Cardiovascular System: A
830 Review. *International Journal of Pediatrics* **2010**, 9 (2010).
- 831 4. Giussani, D.A. The fetal brain sparing response to hypoxia: physiological
832 mechanisms. *The Journal of physiology* **594**, 1215-1230 (2016).
- 833 5. Cohn, H.E., Sacks, E.J., Heymann, M.A. & Rudolph, A.M. Cardiovascular
834 responses to hypoxemia and acidemia in fetal lambs. *Am J Obstet*
835 *Gynecol* **120**, 817-824 (1974).
- 836 6. Giussani, D.A., Spencer, J.A., Moore, P.J., Bennet, L. & Hanson, M.A.
837 Afferent and efferent components of the cardiovascular reflex responses
838 to acute hypoxia in term fetal sheep. *The Journal of physiology* **461**, 431-
839 449 (1993).
- 840 7. Niu, Y., *et al.* Maternal Allopurinol Prevents Cardiac Dysfunction in Adult
841 Male Offspring Programmed by Chronic Hypoxia During Pregnancy.
842 *Hypertension* **72**, 971-978 (2018).
- 843 8. Giussani, D.A., *et al.* Developmental Programming of Cardiovascular
844 Dysfunction by Prenatal Hypoxia and Oxidative Stress. *PLoS one* **7**,
845 e31017 (2012).
- 846 9. Zhang, L. Prenatal Hypoxia and Cardiac Programming. *Journal of the*
847 *Society for Gynecologic Investigation* **12**, 2-13 (2005).
- 848 10. Rueda-Clausen, C.F., Morton, J.S., Lopaschuk, G.D. & Davidge, S.T.
849 Long-term effects of intrauterine growth restriction on cardiac metabolism
850 and susceptibility to ischaemia/reperfusion. *Cardiovascular research* **90**,
851 285-294 (2011).
- 852 11. Xue, Q. & Zhang, L. Prenatal Hypoxia Causes a Sex-Dependent Increase
853 in Heart Susceptibility to Ischemia and Reperfusion Injury in Adult Male
854 Offspring: Role of Protein Kinase C ϵ . *Journal of Pharmacology and*
855 *Experimental Therapeutics* **330**, 624-632 (2009).
- 856 12. Li, G., *et al.* Effect of Fetal Hypoxia on Heart Susceptibility to Ischemia and
857 Reperfusion Injury in the Adult Rat. *Journal of the Society for Gynecologic*
858 *Investigation* **10**, 265-274 (2003).
- 859 13. Patterson, A.J., Chen, M., Xue, Q., Xiao, D. & Zhang, L. Chronic prenatal
860 hypoxia induces epigenetic programming of PKC ϵ gene repression
861 in rat hearts. *Circulation research* **107**, 365-373 (2010).
- 862 14. Shah, A., *et al.* Cardiovascular susceptibility to ϵ PKC in
863 vivo ϵ PKC; ischemic myocardial injury in male and female rat offspring
864 exposed to prenatal hypoxia. *Clinical science* **131**, 2303 (2017).

- 865 15. Beauchamp, B., *et al.* Undernutrition during pregnancy in mice leads to
866 dysfunctional cardiac muscle respiration in adult offspring. *Bioscience*
867 *reports* **35**(2015).
- 868 16. Ferey, J.L.A., *et al.* A maternal high-fat, high-sucrose diet induces
869 transgenerational cardiac mitochondrial dysfunction independently of
870 maternal mitochondrial inheritance. *American journal of physiology. Heart*
871 *and circulatory physiology* **316**, H1202-h1210 (2019).
- 872 17. Larsen, T.D., *et al.* Diabetic Pregnancy and Maternal High-Fat Diet Impair
873 Mitochondrial Dynamism in the Developing Fetal Rat Heart by Sex-
874 Specific Mechanisms. *Int J Mol Sci* **20**, 3090 (2019).
- 875 18. Peng, J., *et al.* The detrimental effects of glucocorticoids exposure during
876 pregnancy on offspring's cardiac functions mediated by hypermethylation
877 of bone morphogenetic protein-4. *Cell Death & Disease* **9**, 834 (2018).
- 878 19. Thompson, L.P., Song, H. & Polster, B.M. Fetal Programming and Sexual
879 Dimorphism of Mitochondrial Protein Expression and Activity of Hearts of
880 Prenatally Hypoxic Guinea Pig Offspring. *Oxidative medicine and cellular*
881 *longevity* **2019**, 7210249 (2019).
- 882 20. Thompson, L.P., Chen, L., Polster, B.M., Pinkas, G. & Song, H. Prenatal
883 hypoxia impairs cardiac mitochondrial and ventricular function in guinea
884 pig offspring in a sex-related manner. *Am J Physiol Regul Integr Comp*
885 *Physiol* **315**, R1232-R1241 (2018).
- 886 21. Al-Hasan, Y.M., Pinkas, G.A. & Thompson, L.P. Prenatal Hypoxia
887 Reduces Mitochondrial Protein Levels and Cytochrome c Oxidase Activity
888 in Offspring Guinea Pig Hearts. *Reproductive Sciences* **21**, 883-891
889 (2014).
- 890 22. Al-Hasan, Y.M., *et al.* Chronic Hypoxia Impairs Cytochrome Oxidase
891 Activity Via Oxidative Stress in Selected Fetal Guinea Pig Organs.
892 *Reproductive Sciences* **20**, 299-307 (2013).
- 893 23. McMillen, I.C. & Robinson, J.S. Developmental origins of the metabolic
894 syndrome: prediction, plasticity, and programming. *Physiological reviews*
895 **85**, 571-633 (2005).
- 896 24. Morrison, J.L. Sheep models of intrauterine growth restriction: fetal
897 adaptations and consequences. *Clinical and experimental pharmacology*
898 *& physiology* **35**, 730-743 (2008).
- 899 25. Allison, B.J., *et al.* Divergence of mechanistic pathways mediating
900 cardiovascular aging and developmental programming of cardiovascular
901 disease. *FASEB journal : official publication of the Federation of American*
902 *Societies for Experimental Biology* **30**, 1968-1975 (2016).
- 903 26. Kane, A.D., Herrera, E.A., Camm, E.J. & Giussani, D.A. Vitamin C
904 prevents intrauterine programming of in vivo cardiovascular dysfunction in
905 the rat. *Circulation journal : official journal of the Japanese Circulation*
906 *Society* **77**, 2604-2611 (2013).
- 907 27. Giussani, D.A. & Davidge, S.T. Developmental programming of
908 cardiovascular disease by prenatal hypoxia. *Journal of Developmental*
909 *Origins of Health and Disease* **4**, 328-337 (2013).

- 910 28. Wolterink-Donselaar, I.G., Meerding, J.M. & Fernandes, C. A method for
911 gender determination in newborn dark pigmented mice. *Lab Anim (NY)* **38**,
912 35-38 (2009).
- 913 29. Deeney, S., Powers, K.N. & Crombleholme, T.M. A comparison of sexing
914 methods in fetal mice. *Lab Anim (NY)* **45**, 380-384 (2016).
- 915 30. Pinali, C., Bennett, H., Davenport, J.B., Trafford, A.W. & Kitmitto, A.
916 Three-Dimensional Reconstruction of Cardiac Sarcoplasmic Reticulum
917 Reveals a Continuous Network Linking Transverse-Tubules. *Circulation*
918 *Research* **113**, 1219-1230 (2013).
- 919 31. Deerinck, T.J., *et al.* Enhancing Serial Block-Face Scanning Electron
920 Microscopy to Enable High Resolution 3-D Nanohistology of Cells and
921 Tissues. *Microscopy and Microanalysis* **16**, 1138-1139 (2010).
- 922 32. Pesta, D. & Gnaiger, E. High-Resolution Respirometry: OXPHOS
923 Protocols for Human Cells and Permeabilized Fibers from Small Biopsies
924 of Human Muscle. Vol. 810 25-58 (Humana Press, Totowa, NJ, 2012).
- 925 33. Lemieux, H., *et al.* Impairment of mitochondrial respiratory function as an
926 early biomarker of apoptosis induced by growth factor removal. *bioRxiv*,
927 151480 (2017).
- 928 34. Spinazzi, M., Casarin, A., Pertegato, V., Salviati, L. & Angelini, C.
929 Assessment of mitochondrial respiratory chain enzymatic activities on
930 tissues and cultured cells. *Nature Protocols* **7**, 1235 (2012).
- 931 35. Lawless, M., *et al.* Phosphodiesterase 5 inhibition improves contractile
932 function and restores transverse tubule loss and catecholamine
933 responsiveness in heart failure. *Scientific Reports* **9**, 6801 (2019).
- 934 36. Briston, S.J., *et al.* Impaired beta-adrenergic responsiveness accentuates
935 dysfunctional excitation-contraction coupling in an ovine model of
936 tachypacing-induced heart failure. *J Physiol* **589**, 1367-1382 (2011).
- 937 37. Caldwell, J.L., *et al.* Dependence of cardiac transverse tubules on the
938 BAR domain protein amphiphysin II (BIN-1). *Circulation research* **115**,
939 986-996 (2014).
- 940 38. Li, R. & Shen, Y. An old method facing a new challenge: re-visiting
941 housekeeping proteins as internal reference control for neuroscience
942 research. *Life Sci* **92**, 747-751 (2013).
- 943 39. Makrecka-Kuka, M., Krumschnabel, G. & Gnaiger, E. High-Resolution
944 Respirometry for Simultaneous Measurement of Oxygen and Hydrogen
945 Peroxide Fluxes in Permeabilized Cells, Tissue Homogenate and Isolated
946 Mitochondria. *Biomolecules* **5**, 1319-1338 (2015).
- 947 40. Puente, B.N., *et al.* The oxygen-rich postnatal environment induces
948 cardiomyocyte cell-cycle arrest through DNA damage response. *Cell* **157**,
949 565-579 (2014).
- 950 41. Chouchani, E.T., *et al.* Ischaemic accumulation of succinate controls
951 reperfusion injury through mitochondrial ROS. *Nature* **515**, 431-435
952 (2014).
- 953 42. Brand, M.D. Mitochondrial generation of superoxide and hydrogen
954 peroxide as the source of mitochondrial redox signaling. *Free Radical*
955 *Biology and Medicine* **100**, 14-31 (2016).

- 956 43. Chen, Y.-R. & Zweier, J.L. Cardiac Mitochondria and Reactive Oxygen
957 Species Generation. *Circulation research* **114**, 524-537 (2014).
- 958 44. Gyllenhammer, L.E., Entringer, S., Buss, C. & Wadhwa, P.D.
959 Developmental programming of mitochondrial biology: a conceptual
960 framework and review. *Proceedings of the Royal Society B: Biological
961 Sciences* **287**, 20192713 (2020).
- 962 45. Dearden, L., Bouret, S.G. & Ozanne, S.E. Sex and gender differences in
963 developmental programming of metabolism. *Molecular Metabolism* **15**, 8-
964 19 (2018).
- 965 46. Botting, K.J., McMillen, I.C., Forbes, H., Nyengaard, J.R. & Morrison, J.L.
966 Chronic hypoxemia in late gestation decreases cardiomyocyte number but
967 does not change expression of hypoxia-responsive genes. *Journal of the
968 American Heart Association* **3**(2014).
- 969 47. Botting, K.J., *et al.* IUGR decreases cardiomyocyte endowment and alters
970 cardiac metabolism in a sex- and cause-of-IUGR-specific manner.
971 *American Journal of Physiology-Regulatory, Integrative and Comparative
972 Physiology* **315**, R48-R67 (2018).
- 973 48. Bae, S., Xiao, Y., Li, G., Casiano, C.A. & Zhang, L. Effect of maternal
974 chronic hypoxic exposure during gestation on apoptosis in fetal rat heart.
975 *Am J Physiol Heart Circ Physiol* **285**, H983-990 (2003).
- 976 49. Wadhwa, P.D., Buss, C., Entringer, S. & Swanson, J.M. Developmental
977 origins of health and disease: brief history of the approach and current
978 focus on epigenetic mechanisms. *Seminars in reproductive medicine* **27**,
979 358-368 (2009).
- 980 50. Gao, Y., *et al.* Multi-Omics Integration Reveals Short and Long-Term
981 Effects of Gestational Hypoxia on the Heart Development. *Cells* **8**, 1608
982 (2019).
- 983 51. Rueda-Clausen, C.F., Morton, J.S. & Davidge, S.T. Effects of hypoxia-
984 induced intrauterine growth restriction on cardiopulmonary structure and
985 function during adulthood. *Cardiovascular Research* **81**, 713-722 (2008).
- 986 52. Hemmings, D.G., Williams, S.J. & Davidge, S.T. Increased myogenic tone
987 in 7-month-old adult male but not female offspring from rat dams exposed
988 to hypoxia during pregnancy. *American Journal of Physiology-Heart and
989 Circulatory Physiology* **289**, H674-H682 (2005).
- 990 53. Larsen, S., *et al.* Biomarkers of mitochondrial content in skeletal muscle of
991 healthy young human subjects. *The Journal of physiology* **590**, 3349-3360
992 (2012).
- 993 54. Bienfait, H.F., Jacobs, J.M. & Slater, E.C. Mitochondrial oxygen affinity as
994 a function of redox and phosphate potentials. *Biochimica et biophysica
995 acta* **376**, 446-457 (1975).
- 996 55. Gnaiger, E. Bioenergetics at low oxygen: dependence of respiration and
997 phosphorylation on oxygen and adenosine diphosphate supply.
998 *Respiration Physiology* **128**, 277-297 (2001).
- 999 56. Dawson, T.L., Gores, G.J., Nieminen, A.L., Herman, B. & Lemasters, J.J.
1000 Mitochondria as a source of reactive oxygen species during reductive

- 1001 stress in rat hepatocytes. *The American journal of physiology* **264**, C961-
1002 967 (1993).
- 1003 57. Duranteau, J., Chandel, N.S., Kulisz, A., Shao, Z. & Schumacker, P.T.
1004 Intracellular signaling by reactive oxygen species during hypoxia in
1005 cardiomyocytes. *J Biol Chem* **273**, 11619-11624 (1998).
- 1006 58. Aiken, C.E. & Ozanne, S.E. Sex differences in developmental
1007 programming models. *Reproduction (Cambridge, England)* **145**, R1-13
1008 (2013).
- 1009 59. Intapad, S., Ojeda, N.B., Dasinger, J.H. & Alexander, B.T. Sex Differences
1010 in the Developmental Origins of Cardiovascular Disease. *Physiology* **29**,
1011 122-132 (2014).
- 1012 60. Ventura-Clapier, R., Piquereau, J., Veksler, V. & Garnier, A. Estrogens,
1013 Estrogen Receptors Effects on Cardiac and Skeletal Muscle Mitochondria.
1014 *Front Endocrinol (Lausanne)* **10**, 557-557 (2019).
- 1015 61. Thornburg, K.L., O'Tierney, P.F. & Louey, S. Review: The placenta is a
1016 programming agent for cardiovascular disease. *Placenta* **31 Suppl**, S54-
1017 S59 (2010).
- 1018 62. Fisher, J.J., Bartho, L.A., Perkins, A.V. & Holland, O.J. Placental
1019 mitochondria and reactive oxygen species in the physiology and
1020 pathophysiology of pregnancy. *Clinical and Experimental Pharmacology
1021 and Physiology* **47**, 176-184 (2020).
- 1022 63. Nuzzo, A.M., *et al.* Placental Adaptation to Early-Onset Hypoxic
1023 Pregnancy and Mitochondria-Targeted Antioxidant Therapy in a Rodent
1024 Model. *The American Journal of Pathology* **188**, 2704-2716 (2018).
- 1025 64. Song, H., Telugu, B.P. & Thompson, L.P. Sexual dimorphism of
1026 mitochondrial function in the hypoxic guinea pig placenta†. *Biology of
1027 Reproduction* **100**, 208-216 (2018).
- 1028 65. Sferruzzi-Perri, A.N., Higgins, J.S., Vaughan, O.R., Murray, A.J. &
1029 Fowden, A.L. Placental mitochondria adapt developmentally and in
1030 response to hypoxia to support fetal growth. *Proceedings of the National
1031 Academy of Sciences of the United States of America* **116**, 1621-1626
1032 (2019).
- 1033 66. Cuffe, J.S.M., *et al.* Mid- to late term hypoxia in the mouse alters placental
1034 morphology, glucocorticoid regulatory pathways and nutrient transporters
1035 in a sex-specific manner. *The Journal of physiology* **592**, 3127-3141
1036 (2014).
- 1037 67. Chen, X., Zhang, L. & Wang, C. Prenatal hypoxia-induced epigenomic and
1038 transcriptomic reprogramming in rat fetal and adult offspring hearts.
1039 *Scientific Data* **6**, 238 (2019).
- 1040 68. Ventura-Clapier, R., *et al.* Mitochondria: a central target for sex differences
1041 in pathologies. *Clinical science* **131**, 803-822 (2017).
- 1042 69. Colom, B., Oliver, J., Roca, P. & Garcia-Palmer, F.J. Caloric restriction
1043 and gender modulate cardiac muscle mitochondrial H₂O₂ production and
1044 oxidative damage. *Cardiovascular research* **74**, 456-465 (2007).
- 1045 70. Moulin, M., *et al.* Sexual Dimorphism of Doxorubicin-Mediated
1046 Cardiotoxicity. *Circulation: Heart Failure* **8**, 98-108 (2015).

- 1047 71. Ribeiro, R.F., *et al.* Sex differences in the regulation of spatially distinct
1048 cardiac mitochondrial subpopulations. *Mol Cell Biochem* **419**, 41-51
1049 (2016).
- 1050 72. Lagranha, C.J., Deschamps, A., Aponte, A., Steenbergen, C. & Murphy, E.
1051 Sex differences in the phosphorylation of mitochondrial proteins result in
1052 reduced production of reactive oxygen species and cardioprotection in
1053 females. *Circulation research* **106**, 1681-1691 (2010).
- 1054 73. Kander, M.C., Cui, Y. & Liu, Z. Gender difference in oxidative stress: a
1055 new look at the mechanisms for cardiovascular diseases. *J Cell Mol Med*
1056 **21**, 1024-1032 (2017).
1057